https://doi.org/10.5194/wes-2021-158
Preprint. Discussion started: 19 January 2022

eawe european academy of wind energy
Open Access WIND ENERGY SCIENCE DISCUSSIONS

The wide range of factors contributing to Wind Resource Assessment accuracy in complex terrain

Sarah Barber[1], Alain Schubiger[1], Sara Koller[2], Dominik Eggli[2], Alexander Radi[3], Andreas Rumpf[4], and Hermann Knaus[4]

[1]Eastern Switzerland University of Applied Sciences, Oberseestrasse 10, 8640 Rapperswil, Switzerland
[2]Meteotest AG, Fabrikstrasse 14, 3012 Bern, Switzerland
[3]Enercon GmbH, 14 E Rue des Clairières, 44840 Les Sorinières, France
[4]Hochschule Esslingen, Kanalstr. 33, 73728 Esslingen am Neckar, Germany

Correspondence: Sarah Barber (sarah.barber@ost.ch)

Abstract. Understanding the uncertainties of Wind Resource Assessments (WRA) is key to reducing project risks, and this is particularly challenging in mountainous terrain. In the academic literature, many complex flow sites have been investigated, but they all focus on comparing wind speeds from selected wind directions, and do not focus on the overall Annual Energy Production (AEP). In this work, a range of simulations are carried out with seven different wind modelling tools at five different complex terrain sites and the results compared to wind speed measurements at validation locations. This is then extended to AEP estimations (without wake effects), showing that wind profile prediction accuracy does not translate directly or linearly to AEP accuracy. This is firstly because there is a surprisingly large variation in energy production calculation techniques between tools, and secondly because the AEP depends strongly upon the relative strength and occurrence of the wind speed in the most commonly-occurring wind direction sectors. This means that the wind model that produces the most accurate wind predictions for a certain wind direction over a certain time period does not always result in the most suitable model for the AEP estimation of a given complex terrain site. In fact, the large number of steps within the WRA process often lead to the choice of wind model being less important for the overall WRA accuracy than would suggest by only looking at wind speeds. It is therefore concluded that it is vitally important for researchers to consider overall AEP - and all the steps towards calculating it - when evaluating simulation accuracies of flow over complex terrain.

https://doi.org/10.5194/wes-2021-158
Preprint. Discussion started: 19 January 2022

eawe european academy of wind energy
Open Access WIND ENERGY SCIENCE DISCUSSIONS

1 Introduction

Understanding the uncertainties of Wind Resource Assessments (WRA) is key to reducing project risks. This is particularly challenging in mountainous terrain, e.g. (Bowen and Mortensen, 1996; Wood, 1995; Pozo et al., 2017), which accounts for around 30% of the world's land surface (Sayre et al., 2018).

Several previous studies examine and compare the performance uncertainties of different wind modelling tools at mountainous, or 'complex' sites, including the Bolund Hill Blind Test (Bechmann et al., 2011; Berg et al., 2011), the Askervain Hill Blind Test (Bao et al., 2018) and the Perdigão field test (Menke et al., 2019; Barber et al., 2020a). However, they are all limited to comparisons of wind speeds for chosen wind directions, or to time periods that are much shorter than those required for WRA. Due to the large number of separate steps, data types and organisations involved in WRAs, it is challenging to accurately and robustly evaluate the accuracy of different tools or workflows for the entire process. A key obstacle is the lack of availability and suitability of relevant validation data.

The only previous studies examining the steps required for full WRAs are the set of 'CREYAP' exercises Mortensen.2015 and a US-based study on Annual Energy Prodution (AEP) errors (Lee and Fields, 2021). CREYAP stands for "Comparison of Resource and Energy Yield Assessment Procedures" and is carried out by Ørsted and the Technical University of Denmark. In the 2021 version, participants estimate the net energy yield for the Walney Extension wind farm, accounting for wind speed variations over time and across the site, and for turbine interaction losses[1]. A summary of the findings from the previous exercises concludes that most of the steps involved in WRA require significant improvement, and the study needs extending for complex terrain effects (Mortensen et al., 2015). The US-based study presents a very valuable literature review of the energy yield assessment errors across the global wind energy industry and provides a summary of how the wind energy industry has been quantifying and reducing prediction errors, energy losses, and production uncertainties (Lee and Fields, 2021). In this work, a long-term trend indicating a reduction in the over-prediction bias was identified. Both of these studies provide valuable information; however, they are limited due to confidentiality issues connected with collecting data from the industry.

The goal of this work is therefore to examine and compare the accuracies of a range of simulations at different complex flow sites in terms of both wind speed and AEP. In order to achieve this, simulations with seven different wind modelling workflows at five different complex terrain sites were carried out, and the resulting wind speeds compared to measurements at a validation location. This was then extended to AEP estimations (without wake effects), and the differences examined. The workflows involved a range of wind modelling tools as well as a range of model set-ups and AEP calculation methodologies.

The paper is organised as follows: the methods applied in this work are described in Section 2, the results in terms of wind speed are presented in Section 3, the results are extended to AEP in Section 4, and the conclusions are discussed in Section 5.

[1] https://windeurope.org/tech2021/creyap-2021/

https://doi.org/10.5194/wes-2021-158
Preprint. Discussion started: 19 January 2022

eawe european academy of wind energy
Open Access WIND ENERGY SCIENCE DISCUSSIONS

2 Applied methods

2.1 The applied workflows

In this paper, the simulation set-ups are referred as 'workflows' to highlight the fact that each AEP estimation contains an entire workflow, i.e. many steps as well as the wind modelling part. For each workflow, the digital topography and surface roughness data for each site was downloaded from the satellite observation Copernicus database[2].

2.1.1 Underlying wind models

The workflows applied were associated with different wind models as follows:

- **WF-1: WindPro**: The industry-leading software suite for design and planning of wind farm projects[3]. It allows calibration data to be entered directly at the mast location and splits the flow into a total of 12 wind direction sectors. The turbulence intensity is calculated directly from the input met mast data standard deviations and mean values.

- **WF-2: WindSim**: An industry software using a Computational Fluid Dynamics (CFD) model based on the PHOENICS code, a 3D Reynolds Averaged Navier Stokes (RANS) solver from the company CHAM. It allows calibration data to be entered directly at the mast location and splits the flow into a total of 12 wind direction sectors. The turbulence intensity is calculated directly from the input met mast data standard deviations and mean values. In this work, the simulations were conducted using the standard k-ϵ turbulence model (Rodi and Spalding, 1983). The boundary condition at the top was fixed pressure.

- **WF-3: ANSYS CFX**: An all-purpose CFD software. In this work, ANSYS CFX (version 19.2) was applied using an Unsteady RANS approach in combination with the k-ϵ model (Richards and Hoxey, 1993). The equation system was extended to an anelastic formulation whereby the density is influenced by buoyancy forces using the Boussinesq approximation (Montavon, 1998). The Earth's rotation was considered with additional terms in the momentum equation to describe the Coriolis force at a given angular velocity. Forested areas were considered through a canopy model (Liu et al., 1996). Individual roughness lengths of the canopy were attributed to each land use and are chosen according to the work of Wieringa (Wiernga, 1993). These methods have previously been applied successfully to other applications (Knaus et al., 2017). Static boundary conditions were applied around the resolved volume for the chosen wind direction and wind speed, forming a Taylor Spiral. Since the upper boundary condition of the domain is flat, but the ground surface is not, the mass flow rate was balanced at the top surface of the domain in order to prevent an acceleration due to mass conservation of the setup. Turbulence was introduced by entering a turbulence intensity of 10% as an input condition. In order to match the WindPro and WindSim simulations, a total of 12 wind direction sectors were simulated.

[2]https://land.copernicus.eu/
[3]www.wasp.dk

https://doi.org/10.5194/wes-2021-158
Preprint. Discussion started: 19 January 2022

eawe european academy of wind energy
Open Access WIND ENERGY SCIENCE DISCUSSIONS

- **WF-4: Fluent RANS**: ANSYS Fluent is a commercial CFD tool for modelling the flow in industrial applications and can be set up to solve the RANS equations, as well as for the Large Eddy Simulations (LES) or Detached Eddy Simulations (DES) approach. In this work, Fluent was first set up to solve the RANS equations with the SST k-ω turbulence model (Menter, 2012). The inlet wind speed profiles, turbulent kinetic energy and turbulent dissipation rate were imposed based on the roughness height according to Richards and Hoxey (1993). In order to match the WindPro and WindSim simulations, a total of 12 wind direction sectors were simulated.

- **WF-5: Fluent SBES**: A technique within ANSYS Fluent called "Stress-Blended Eddy Simulation" (SBES) was applied. SBES is a new model that offers improved shielding of RANS boundary layers and a more rapid RANS-LES "transition", amongst other things. The RANS results were used to initialise SBES, which was performed unsteadily with an adaptive time stepping procedure ensuring CFL <= 1. After an additional unsteady initialisation, the wind speeds were averaged over 10 minutes. The wind rose measured at the met mast was used to choose the main wind directions, and only these directions were simulated. In order to introduce fluctuating velocities at the inlet, the Fluent Synthetic Turbulence Generator was used. In order to save computational power, all 12 wind direction sectors were not simulated. Instead, only the most frequently occurring sectors were simulated, and Fluent RANS results were used for the other sectors. For workflow WF-5a, three sectors were simulated with SBES and for workflow WF-5b, seven sectors were simulated with SBES.

- **WF-6: PALM**: The model PALM is based on the non-hydrostatic, filtered, incompressible Navier-Stokes equations in Boussinesq-approximated form (an anelastic approximation is available as an option for simulating deep convection). Furthermore, an additional equation is solved for either the subgrid-scale turbulent kinetic energy using Large-Eddy Simulations (LES)[4]. In this work, due to the long computational time, not all sectors could be simulated. Instead, the most frequent sectors were simulated and complemented with the WindSim simulations. The TKE-1 Turbulence Model was applied.

- **WF-7: E-Wind**: E-Wind solves the 3D RANS equations, with a modified k-ϵ turbulence closure. The governing equations are implemented in the open source toolbox OpenFOAM.

2.1.2 Simulation calibration

For each site, measurement data was available for at least two different locations, and the most available and reliable data at the location closest to the planned or existing wind turbine hub height(s) was chosen for calibration. For WindPro and WindSim, the calibration data could be directly input into the tool. For the CFD simulations, the calibration was undertaken for each wind direction sector simulated by inputting a generic logarithmic wind profile calculated using the roughness height value at the simulation input location (Richards and Hoxey, 1993), and then scaling the simulation results by a constant calibration factor, defined as the ratio between the simulated and the long-term corrected measured wind speed at the calibration location.

[4]https://palm.muk.uni-hannover.de/trac/wiki/palm

https://doi.org/10.5194/wes-2021-158
Preprint. Discussion started: 19 January 2022

2.1.3 Simulation validation

For each site, the second measurement point was taken for the validation. The validation was carried out by first calculating the wind speed and direction at the validation location for each calibrated wind direction sector simulation, and then by comparing these values to the measurements.

2.1.4 Wind speed long-term extrapolation

For each site, the long-term corrected measured wind speed was obtained at both the calibration and validation locations by firstly averaging the wind speeds over a time period for which valid data was available for both the calibration and validation measurements. Secondly, these average wind speeds were extrapolated for a 20-year period using the Measure-Correlate-Predict method with long-term reference data. This data was either obtained from a nearby met mast or from MERRA-2 data[5], as discussed in each individual section.

2.1.5 AEP calculation

The wind industry tools applied in this work, WindPro and WindSIM, as well as E-Wind (Alletto et al., 2018), offer a user interface containing all the steps required to get from wind measurements to AEP predictions. However, the other CFD tools, Fluent, CFX and PALM needed to be extended in order to calculate the AEP. In previous work (Barber et al., 2020b), automated workflows for carrying out wind flow modelling in complex terrain were developed for the commercial CFD tools ANSYS Fluent and ANSYS CFX. These processes included a pre-processing tool, a meshing script, a simulation script and a post-processing tool. It was shown that the total simulation costs, including model set-up and post-processing effort costs, could be reduced by a factor of 12 for Fluent and seven for CFX through this automation. For PALM, a slightly different method was applied in order to reduce the computational time in a pragmatic way. This involved firstly searching for a time period in the met mast data for which the wind speed remained relatively stable at the average wind speed for each wind direction sector. For this time period, COSMO-D2 data[6] was taken for the PALM boundary conditions by reading the data from a dynamic input file (offline nesting). Finally, this time period is simulated with PALM and the average wind speed is extracted for the calibration and validation positions at the reference height.

In the present work, these workflows were extended to include AEP estimations. The AEP was calculated at the validation location(s) as follows:

- Speed-up factors between the validation location(s) and the calibration location were calculated from the simulation results for each wind direction sector (in this case, 12 sectors).
- Option 'Time-series method':

[5]https://gmao.gsfc.nasa.gov/reanalysis/MERRA-2/
[6]http://www.cosmo-model.org/content/tasks/operational/dwd/default$_d2.htm$

https://doi.org/10.5194/wes-2021-158
Preprint. Discussion started: 19 January 2022

eawe european academy of wind energy
Open Access WIND ENERGY SCIENCE DISCUSSIONS

  - The amount of wind turning between the validation location(s) and the calibration location was calculated from the simulation results for each wind direction sector.
  - Based on the wind direction sector, each measured ten-minute averaged wind speed at the calibration location was multiplied by the relevant speed-up factor to obtain the expected wind speed at the validation location for that ten minute period.
  - For sectors with a wind direction turning larger than +/- 15°, each data point was moved to the relevant new sector.
  - The linearly-interpolated bin-averaged power curve provided by the manufacturer with $1\ \mathrm{ms}^{-1}$ wide bins was used to obtain the expected power production for every ten-minute wind speed at the validation location(s). For this, it was assumed that the wind speed at the validation location remained constant over the entire wind turbine rotor area. The Rotor Equivalent Wind Speed was not used because the commercial tools do not use this method and a fair comparison was required.
  - These powers were each multiplied by 10/60 hours (10 minutes) and added up to obtain the total energy production over the measurement period.

- Option 'Weibull method':
  - A frequency distribution of the calibration location data for was created for each sector.
  - A Weibull distribution was fitted to each frequency distribution.
  - The Weibull distributions were scaled for each sector using the simulated speed-up factors. The shape factor was kept constant.
  - The scaled Weibull distributions were multiplied by the bin-averaged power curve provided by the manufacturer with 1 m/s wide bins to obtain the total energy production over the measurement period.
- The total energy production was converted to AEP by scaling the energy production in each wind direction sector linearly with the total measurement time.

The three research partners in this project created their own separate workflows for this AEP calculation. For validation purposes, the workflows were firstly compared to each by entering the same simulation results from the WindSim model at one site (Site 1, see description in Section 2.2). An overview of the results is shown in Table 1. As well as comparing the results between organisations, the 'Time-series method' and the 'Weibull method' are compared. Finally, the effect of interpolating the power curve or simply using the $1\ \mathrm{ms}^{-1}$ wide bins is compared.

The variation between the results of different partners is less than 5%, giving us a general confidence in the methods. The largest variation is between the 'Weibull method' and the 'Time series method' (3.4% for the OST method). The difference between the power curve bins and the interpolation is small (1.2% for the OST method, 0.6% for the HSE method, 0.1% for the WindSim method). It should be noted that 5% is not an insignificant amount of energy, and the variations between methods are surprising to the authors. A significant effort in comparing the methods and correcting small errors did not lead to a reduction in these differences.

https://doi.org/10.5194/wes-2021-158
Preprint. Discussion started: 19 January 2022

eawe european academy of wind energy
Open Access WIND ENERGY SCIENCE DISCUSSIONS

Table 1. Summary of AEP comparisons for the different methods used in this paper

Calculation number	Organisation	Method	Power curve	AEP (kWh)
1	OST	Weibull	Bins	1,124,125
2	OST	Time series	Bins	1,073,634
3	HSE	Time series	Bins	1,059,076
3.1	HSE	Time series	Interpolated	1,067,386
4	WindSim	Time series	Bins	1,075,354
4.1	WindSim	Time series	Interpolated	1,075,830
5	WindSim	Weibull	Bins	1,107,025
5.1	WindSim	Weibull	Interpolated	1,065,270
6	Meteotest	Time series	Bins	1,179,359
6.1	Meteotest	Time series	Interpolated	1,174,415

2.2 The simulated sites

An overview of the simulated sites is shown in Fig. 1, except for Site 5, which is confidential. The details and the workflow set-ups for each site are described in the individual sections below.

2.2.1 Site 1

Site 1 is a complex terrain, partly-forested site close to Stoetten in southern Germany, whose central feature is a steep incline above 30% and a main wind direction of 270°-300°. Wind speed and direction data was available from a met mast located about 1 km away from the incline, as well as a lidar, as described in (Schulz et al., 2014). In this paper, the met mast data from four cup anemometers with an accuracy of 1% and three 3D sonic anemometers with an accuracy of 1.5% were used for calibration, and the wind speed data recorded using the SWE-Scanner, a fast pulsed lidar wind scanner based on a Leosphere Windcube V1 system with an adapted scanner unit, were used for validation. The coordinates of the calibration location are (4309721.715, 2838928.447) (coordinate system EPSG3035). For the measurement campaign used in this work, the lidar was positioned approximately 300 m west of the met mast for approximately one year (March 2015 - February 2016). An overview of the site and the wind rose from the met mast at 98 m over the entire measurement period are shown in Fig. 1. S&G Engineering SG750.54 wind turbines with a hub height of 100 m are planned at the site. For the long-term extrapolation, measurement data from the station Stoetten of the German weather service DWD was used. The details of the applied workflows are shown in Table 2. WF-7 was not applied to this site.

https://doi.org/10.5194/wes-2021-158
Preprint. Discussion started: 19 January 2022

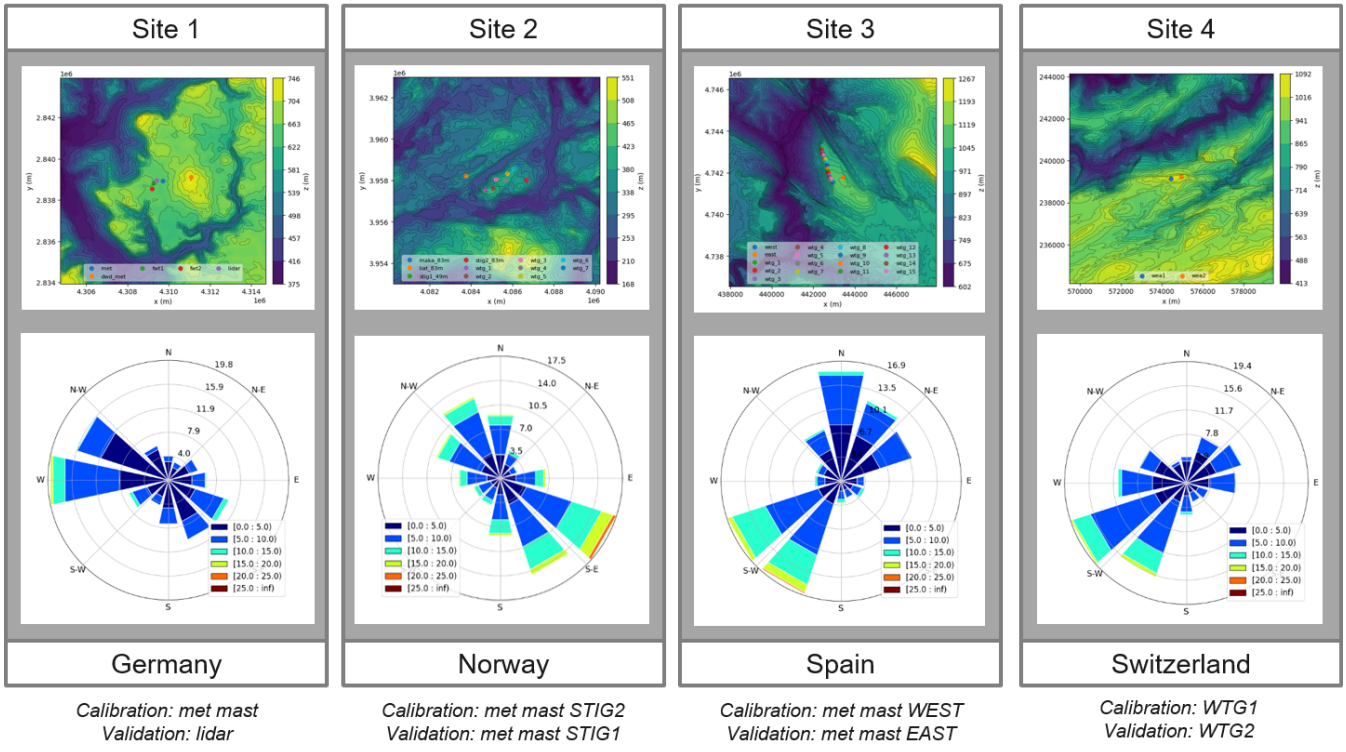

Figure 1. An overview of four of the five sites simulated in this work (Site 5 is confidential): (a) Site 1, (b) Site 2, (c) Site 3 and (d) Site 4

2.2.2 Site 2

Site 2 is an existing wind farm site in Norway surrounded by a terrain of hills, lakes and forests. The wind farm consists of seven Siemens SWT-DD-130 wind turbines with a hub height of 115 m located on a small hill as shown on Fig. 1. The circles on this figure refer to met masts and wind turbines. Another wind farm consisting of 22 wind turbines is located on the hill to the north of the wind farm. The two main wind directions are SE and NW, as can be seen on the wind rose from the met mast STIG2 in Fig. 1. In this project, the two met masts close to the wind turbines, 'STIG1' and 'STIG2', are used. For STIG1, wind speed measurement data is available from Thies First Class Cup Anemometers at five heights up to 50 m from June 2007 to May 2016 (9 years). For STIG2, wind speed measurement data from cup anemometers is available at five heights up to 83 m from December 2013 to January 2016 (2 years). STIG1 has three sensors at very similar heights (48 m, 49 m and 50 m), whereas STIG2 has two sensors at similar heights (82 m and 83 m). An examination of the time series of the measurement data showed that the sensors at 47 m, 48 m and 82 m contained some errors, and therefore the sensors at these heights were not used. STIG2 at 83 m is taken as the calibration mast, with coordinates of (4086674.443, 3958009.528) (coordinate system EPSG3035). For the long-term extrapolation, MERRA-2 data was. The details of the applied workflows are shown in Table 3. WF-3 and WF-7 were not applied to this site.

https://doi.org/10.5194/wes-2021-158
Preprint. Discussion started: 19 January 2022

eawe european academy of wind energy
Open Access WIND ENERGY SCIENCE DISCUSSIONS

2.2.3 Site 3

Site 3 is an existing wind farm site in Spain situated in complex terrain. The wind farm consists of 15 Enercon E-40 wind turbines with a hub height of 50 m located at the top of a steep ridge as shown in Fig. 1. The circles on this figure refer to met masts and wind turbines. The two main wind directions are E and NNW, as can be seen on the wind rose in Fig. 1. In this project, data from two met masts 'EAST' and 'WEST' were used. For both of these masts, measurement data was provided from Thies First Class Cup Anemometers at a range of heights up to 50 m from September 2009 to September 2010. Due to the high amount of overlapping data points (48,941), they can be used for the calibration and validation data reliably. The MERRA-2 reanalysis dataset was used for the long-term adjustment of both met mast data sets. From the MERRA-2 data, a factor of the mean wind speed during 10 years to the mean wind speed over the measurement period was determined. For the long-term adjusted data sets at both locations, the measurement series were extrapolated with this factor. The WEST mast was used for calibration and the EAST mast for validation. The coordinates of the calibration location are (442929.200, 4741536.600) (coordinate system EPSG3035). The details of the applied workflows are shown in Table 4. All seven workflows were applied to this site.

2.2.4 Site 4

Site 4 is the existing St. Brais wind farm site in Switzerland situated in complex terrain. The wind farm consists of two Enercon E-82 wind turbines with a hub height of 78 m located as shown in Fig. 1. The main wind direction is NW, as can be seen on the wind rose on the figure. In this project, wind speed and direction data from the two wind turbines 'WEA1' and 'WEA2' were used, because no met mast data was available. The measurement location on the nacelle of the wind turbines (hub height 78 m) means that the data will be influenced by the wind turbine rotors, and the measurements will not correspond to the freestream wind speed. It is not known if the measurement data include any kind of correction for this effect or not. However, it is nevertheless possible to use one wind turbine as the calibration location and the other as the validation location. The absolute values of the wind speeds may not be correct, but the ratios will still be valid, assuming that there are no large discrepancies in the operation of the wind turbines. For both of these wind turbines, measurement data was provided from January 2010 to December 2020, a time period of 10 years. Due to the high amount of overlapping data points (554,045), they can be used for the calibration and validation data reliably. A long-term extrapolation was not done because the measurement period is already very long. The wind turbine WEA1 was used for calibration and WEA2 for validation. The coordinates of the calibration location are (574452.000, 239147.000) (coordinate system EPSG21781). A good correlation between the WEA1 and WEA2 data could be seen. The details of the applied workflows are shown in Table 5. Neither WF-3 nor WF-6 were applied.

2.2.5 Site 5

Site 5 is a planned site that cannot be described in detail here for confidentiality reasons. However, the results are still included in this work in the form of comparisons. The site is located in hilly terrain. Data from two met masts over a time period of six months is available. Long-term corrections were made using nearby weather station reference data. The met mast closest to the

https://doi.org/10.5194/wes-2021-158
Preprint. Discussion started: 19 January 2022

eawe european academy of wind energy
Open Access WIND ENERGY SCIENCE DISCUSSIONS

planned wind turbines was chosen for the calibration point. The details of the applied workflows are shown in Table 6. Neither WF-3 nor WF-6 were applied.

Table 2. Set-up of the workflows at Site 1

Criteria	WF-1	WF-2	WF-3	WF-4	WF-5	WF-6
Wind model	WindPro	WindSim	CFX	Fluent RANS	Fluent SBES	PALM
Grid dimensions	9x9 km	9x9x5 km	20x22x2.5 km	10x10x1.5 km	10x10x1.5 km	6x6x6.5 km
Horizontal resolution	25 m	25 m	25 m	20 m	20 m	10 m
Number of cells	129,600	4.5m	17m	20m	20m	54m

Table 3. Set-up of the workflows at Site 2

Criteria	WF-1	WF-2	WF-4	WF-5	WF-6
Wind model	WindPro	WindSim	Fluent RANS	Fluent SBES	PALM
Grid dimensions	25x25 km	5x5x5 km	10x10x1.5 km	10x10x1.5 km	20x10x4 km
Horizontal resolution	25 m	25 m	20 m	20 m	20 m
Number of cells	1.0m	1.9m	20m	20m	1.6m

Table 4. Set-up of the workflows at Site 3

Criteria	WF-1	WF-2	WF-3	WF-4	WF-5	WF-6	WF-7
Wind model	WindPro	WindSim	CFX	Fluent RANS	Fluent SBES	PALM	E-Wind
Grid dim.	20x20 km	10x10x8 km	20x20x4 km	10x10x1.5 km	10x10x1.5 km	18x18x10 km	20 km dia.
Hor. res.	25 m	25 m	25 m	20 m	20 m	25 m	50 m
No. cells	640,000	13.8m	1.6m	20m	20m	17.6m	600,000

https://doi.org/10.5194/wes-2021-158
Preprint. Discussion started: 19 January 2022

eawe european academy of wind energy
Open Access WIND ENERGY SCIENCE DISCUSSIONS

Table 5. Set-up of the workflows at Site 4

Criteria	WF-1	WF-2	WF-4	WF-5
Wind model	WindPro	WindSim	Fluent RANS	Fluent SBES
Grid dimensions	9x9 km	10x10x10 km	10x10x1.5 km	10x10x1.5 km
Horizontal resolution	25 m	25 m	20 m	20 m
Number of cells	129,600	10.2m	20m	20m

Table 6. Set-up of the workflows at Site 5

Criteria	WF-1	WF-2	WF-4	WF-5
Wind model	WindPro	WindSim	Fluent RANS	Fluent SBES
Grid dimensions	9x9 km	10x10x10 km	10x10x1.5 km	10x10x1.5 km
Horizontal resolution	25 m	25 m	20 m	20 m
Number of cells	129,600	10.2m	20m	20m

https://doi.org/10.5194/wes-2021-158
Preprint. Discussion started: 19 January 2022

3 Simulation results - wind speeds

For each site, a total of 12 simulations were carried out - one for each 30° wind direction sector. In this section, the simulation results are shown in terms of absolute differences between the measurements and simulations at the calibration and validation locations for each site. For locations with data at more than one height, the Root Mean Square Error of all measured heights compared to simulations is used as a comparison.

Detailed simulation results for each site can be found in the final project report (Barber et al., 2001). This includes speed-up factors and turning between calibration and validation locations, comparisons of simulated and measured wind speed and direction profiles for all wind directions and wind speed contours.

3.1 Site 1

The average RMSE values between the simulations and the measurements over all 12 wind direction sectors are shown in Fig. 2. The top row ((a) and (b)) shows the calibration location and the bottom row ((c) and (d)) the validation location. The left-hand plots ((a) and (c)) show the results of a simple averaging of the RMSE values over the 12 wind direction sectors, whereas the right-hand plots ((b) and (d)) show RMSE averages weighted for the wind speed frequency distribution measured at the calibration location. This weighted averaging gives more weighting to more frequent wind speeds in an attempt to provide a number more relevant for the AEP. For this site, it can be seen that the weighted averaging does not have a large effect on the results. This indicates that the errors of the most frequent wind directions are close to the average value.

The different bars in each plot represent different measurement heights that have taken to calculate the RMSE, with the number of points increasing with increasing darkness of the colours. The light green colour refers to just one point and therefore the RMSE is equal to the absolute difference between measured and simulated wind speed. This number is very low for the calibration location as expected.

For the calibration location, the variable 'RMSE 25-100m' refers to the RMSE value using all the measurement heights except for the lowest point, because this point is difficult to simulate accurately and also less relevant for the AEP calculation as it is not inside the rotor area of the planned wind turbines. 'RMSE 10-100m' refers to the RMSE value using all the measurement heights. The values increase with an increasing number of points, because the simulations become less accurate close to the ground. This is expected, especially for heights below 25 m. In general, the results at the calibration location indicate that the wind speed profile has not been captured well for all workflows, even if the lower points are removed.

For the validation location, the variable 'RMSE 75-125m' refers to the RMSE value using only the heights within the rotor area of the planned wind turbines, and 'RMSE 50-150m' refers to the RMSE value using all the measurement heights. The values increase with an increasing number of points, because the simulations become less accurate close to the ground. This is expected, especially for heights below 25 m. However, this effect is not as large as for the calibration location. In general, the entire profile is predicted fairly inaccurately, which is surprising due to the close location of the calibration and validation location (see Fig. 1). Another thing to notice about the RMSE values at the validation location is the particular low accuracy of WF-1 (WAsP) compared to the other workflows.

https://doi.org/10.5194/wes-2021-158
Preprint. Discussion started: 19 January 2022

eawe european academy of wind energy
Open Access WIND ENERGY SCIENCE DISCUSSIONS

3.2 Site 2

For Site 2, measurement data was only available at one height. Therefore the average absolute differences between the measurements and simulations over all 12 wind direction sectors at (a) the calibration location and (b) the validation location at hub height are shown in Fig. 3. The different bar colours represent simple and weighted averaging of the wind direction sectors, as introduced in the previous section. The error at the calibration location is very small, remaining below $0.006\,\mathrm{ms}^{-1}$ for each workflow. For the validation location, the errors all remain below $1\,\mathrm{ms}^{-1}$. WF-1 (WindPro) and WF-2 (WindPro) are closer to the measurements than WF-4 (CFX), WF-5 (Fluent) and WF-6 (PALM). The weighted averaging affects both WF-1 (WindPro) and WF-2 (WindPro), but for WF-1 it increases the error and for WF-2 it decreases the error. The reason for this is not clear and is investigated in Section 4.

3.3 Site 3

For Site 3, measurement data was only available at one height. Therefore the average absolute differences between the measurements and simulations over all 12 wind direction sectors at (a) the calibration location and (b) the validation location are shown in Fig. 4. For the calibration location, the errors for all workflows are all below $0.08\,\mathrm{ms}^{-1}$, which are due to extrapolation errors in the calibration method. For the validation location, the errors all remain below $1\,\mathrm{ms}^{-1}$, as for Site 2. However, the difference between workflows is less significant. WF-4 (CFX) and WF-5 (Fluent) are generally more accurate. The weighted averaging generally has a small influence on the results.

3.4 Site 4

For Site 4, measurement data was only available at one height. Therefore the average absolute differences between the measurements and simulations over all 12 wind direction sectors at (a) the calibration location and (b) the validation location are shown in Fig. 5. For the calibration location, the errors for all workflows are all below $0.06\,\mathrm{ms}^{-1}$, which are due to extrapolation errors in the calibration method. For the validation location, the errors are even lower than the previous sites, remaining below $0.5\,\mathrm{ms}^{-1}$. Similarly to Site 2, WF-1 (WindPro) and WF-2 (WindPro) are closer to the measurements than WF-4 (CFX) and WF-5 (Fluent). Again, the weighted averaging generally has a small influence on the results.

3.5 Site 5

For Site 5, measurement data was only available at one height. Therefore the average absolute differences between the measurements and simulations over all 12 wind direction sectors at (a) the calibration location and (b) the validation location are shown in Fig. 6. For the calibration location, the errors for all workflows are all below $0.02\,\mathrm{ms}^{-1}$, which are due to extrapolation errors in the calibration method. For the validation location, the errors are similar to Sites 1-3, remaining between $0.5\,\mathrm{ms}^{-1}$ and $1\,\mathrm{ms}^{-1}$. Similarly to Site 3, the difference between the workflows is not very large. However, the effect of the weighted averaging is not insignificant. This was found to be because the largest deviations from the measurements occurred at the more frequent wind speeds, and is discussed further in Barber et al. (2001).

https://doi.org/10.5194/wes-2021-158
Preprint. Discussion started: 19 January 2022

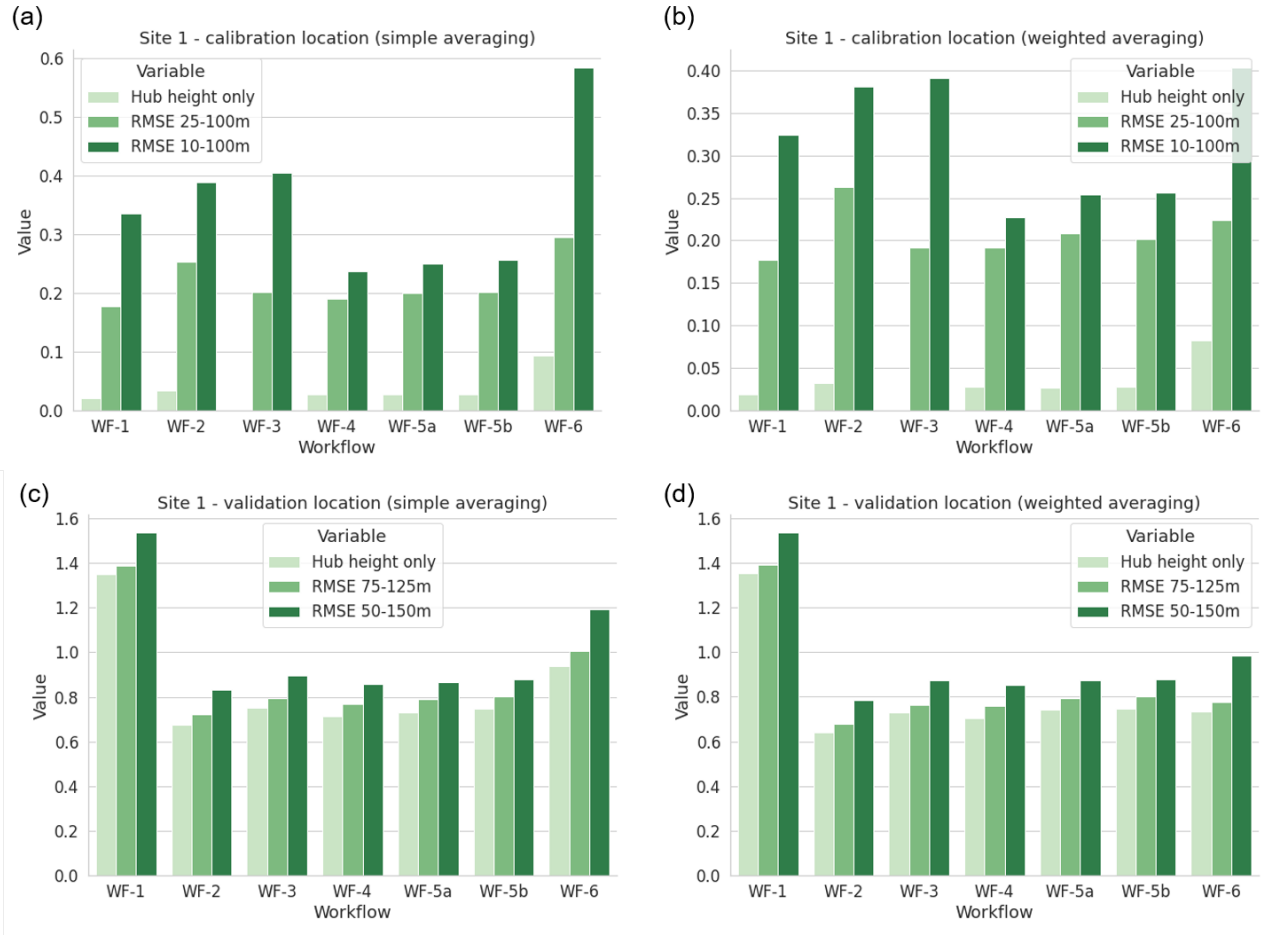

Figure 2. Site 1 - RMSE values between the measurements and simulations at (a) the calibration location and (b) the validation location for different numbers of measurement heights, for simple and weighted wind direction sector averaging (ms^{-1})

https://doi.org/10.5194/wes-2021-158
Preprint. Discussion started: 19 January 2022

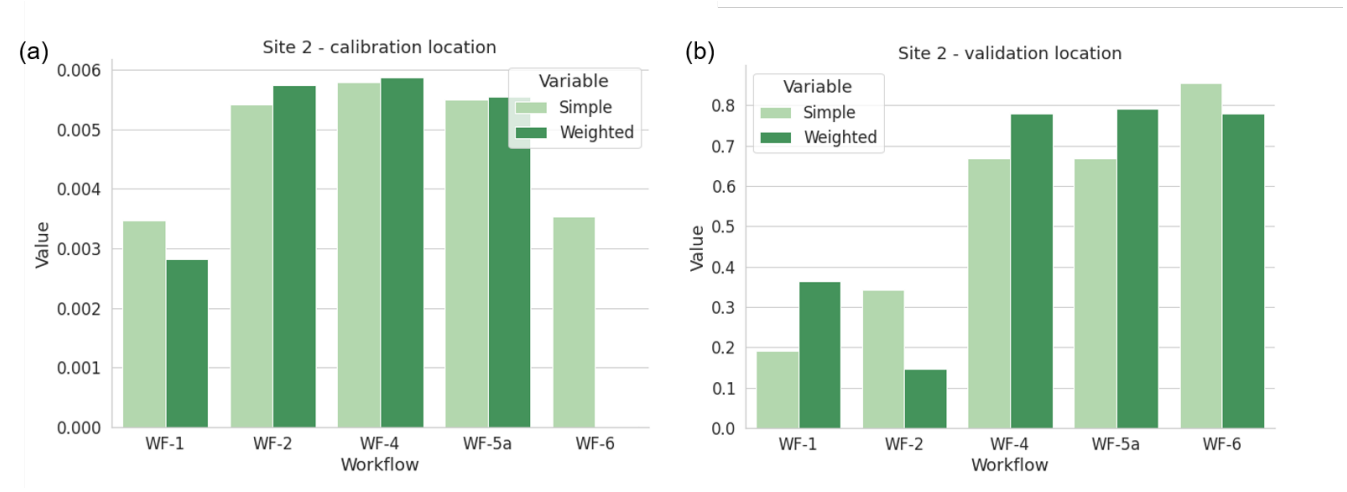

Figure 3. Site 2 - absolute differences between the measurements and simulations at (a) the calibration location and (b) the validation location (ms^{-1})

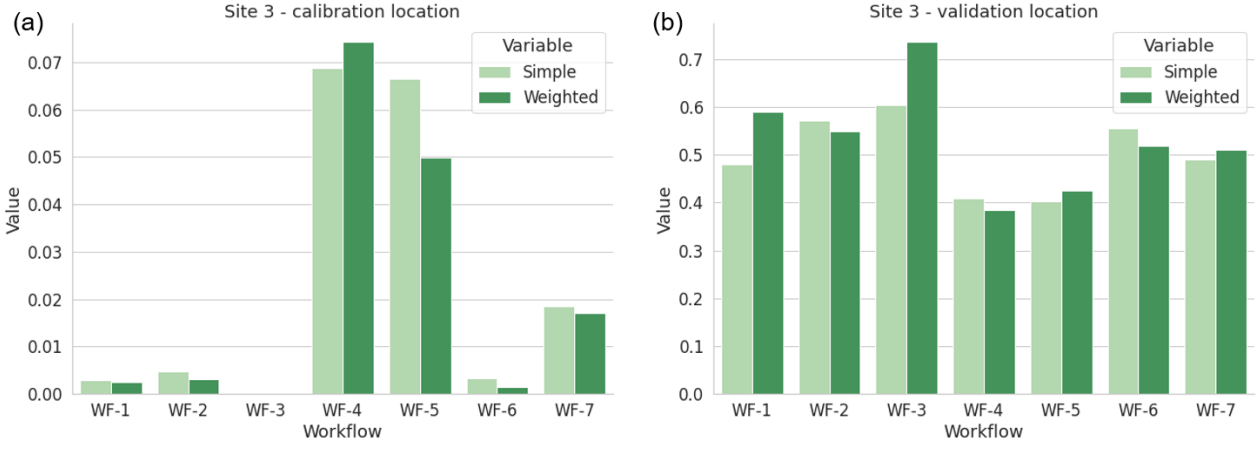

Figure 4. Site 3 - absolute differences between the measurements and simulations (a) the calibration location and (b) the validation location (ms^{-1})

https://doi.org/10.5194/wes-2021-158
Preprint. Discussion started: 19 January 2022

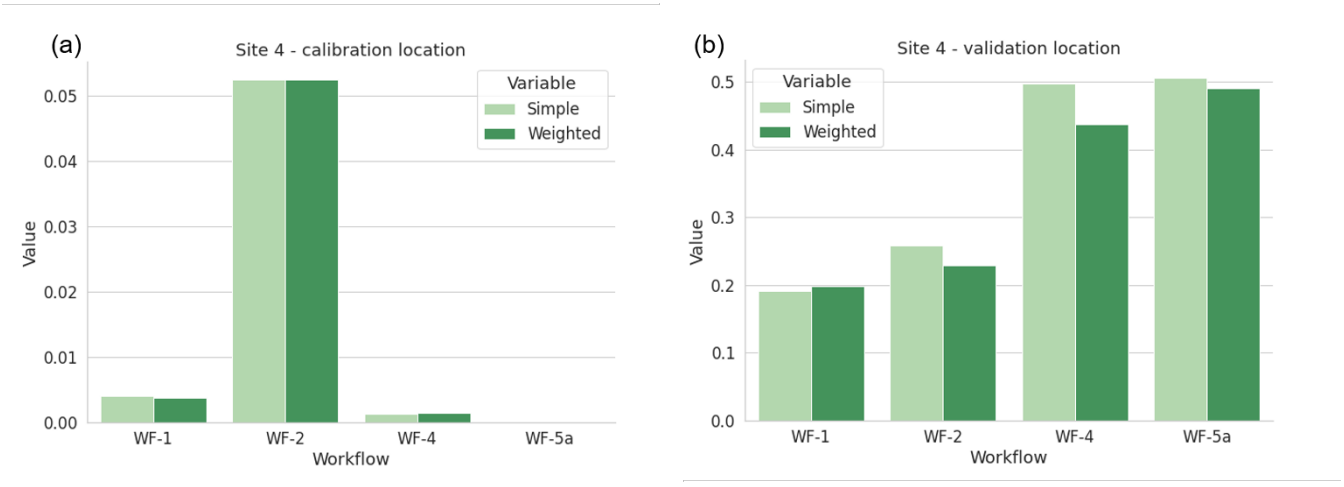

Figure 5. Site 4 - absolute differences between the measurements and simulations at (a) the calibration location and (b) the validation location (ms^{-1})

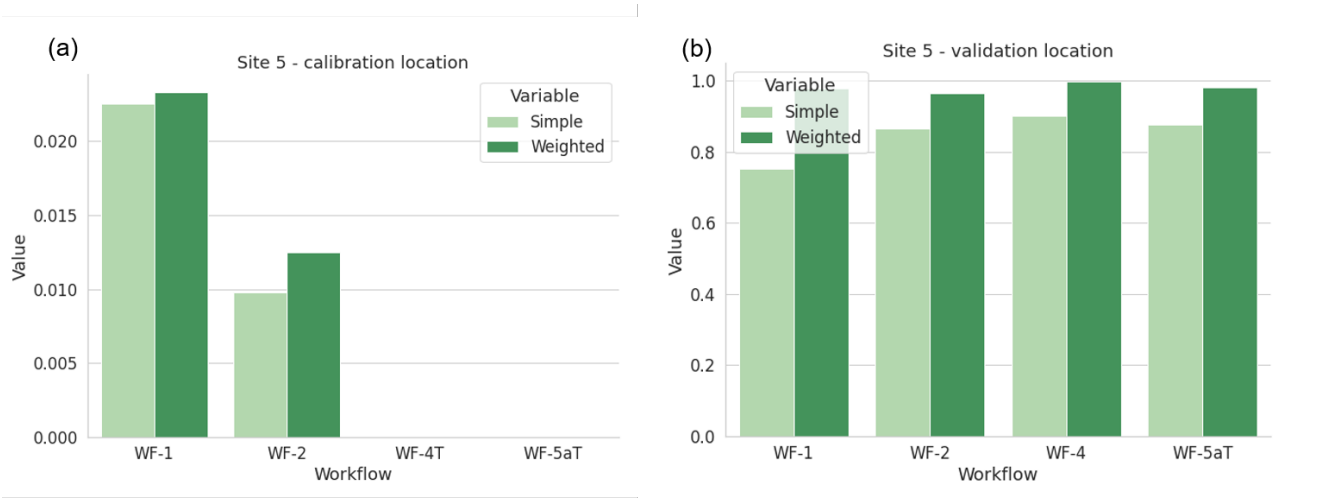

Figure 6. Site 5 - absolute differences between the measurements and simulations at (a) the calibration location and (b) the validation location (ms^{-1})

https://doi.org/10.5194/wes-2021-158
Preprint. Discussion started: 19 January 2022

eawe european academy of wind energy
Open Access WIND ENERGY SCIENCE DISCUSSIONS

4 Simulation results - Annual Energy Production (AEP)

In this section, the results at the validation location for each site are shown in terms of AEP, which was calculated site from the simulation results for each workflow as described in Section 2. There are no AEP measurements to compare the results with, so instead each result was compared to a 'theoretical' value of AEP. This was determined using the AEP 'Time-series method' described in Section 2.1.4, but instead of using the simulation results to scale the calibration data time series, the measured time series as the validation location was used directly. This allowed the effect of the simulated differences in wind speeds to be transferred to differences in AEP. Throughout this work, AEP refers to the gross production, i.e. without any losses or wake effects.

4.1 Site 1

The wind turbine chosen for the AEP calculation at the validation location of Site 1 was a S&G Engineering SG750.54 with a hub height of 100 m, because this is the type planned for this site (construction planned in 2022). This wind turbine has a rated power of 750 kW and a rated wind speed of 11 m/s. In order to calculate the AEP, each research partner implemented their own script according to the 'Time series method' described in Section 2.1.4. The results are shown in Fig. 7 in terms of the percentage differences from the 'theoretical' value. All the results are significantly lower than the theoretical value. The differences in AEP are due to the differences in simulation results as well as the differences in the AEP methods between research partners. For WF-3 (CFX), a comparison was additionally made with and without the effects of turning (as described in Section 2.1.4). WF-3T in the figure refers to the calculating with the consideration of turning effects. A very small difference was observed. Details of the variations of the AEP for each wind direction sector can be found in Barber et al. (2001). It was found that a large variation between model and sector exists, without a particular trend.

4.2 Site 2

For this site, the AEP has been calculated at the validation location using the power curve of the Siemens SWT-DD-130 wind turbine. A hub height of 50 m instead of the real hub height of 115 m was used in order to avoid additional inaccuracies due to the wind speed profile vertical extrapolation. This wind turbine has a rated power of 3.9 MW and a rated wind speed of 13 m/s. The results in Fig. 8 show that the results match very well for WF-1 (WindPro), WF-2 (WindSIM), WF-4 (Fluent RANS) and WF-5a (Fluent SBES), with deviations less than 3%. The WF-6 (PALM) result is significantly lower, with a deviation of 32%. This is due to the under-predicted wind speed shown in Section 3.

Details of the variations of the AEP for each wind direction sector can be found in Barber et al. (2001). It was found that the AEP was under-predicted in the three most frequent sectors (120°, 270° and 300°), leading to an overall under-prediction of AEP. For WF-6 (PALM), the 270° and 300° sectors are especially strongly under-predicted, explaining the large deviation compared to the theoretical AEP.

https://doi.org/10.5194/wes-2021-158
Preprint. Discussion started: 19 January 2022

eawe european academy of wind energy
Open Access WIND ENERGY SCIENCE DISCUSSIONS

4.3 Site 3

For this site, the AEP has been calculated at the validation location using the power curve of the Enercon E-40 wind turbine. This wind turbine has a rated power of 0.6 MW and a rated wind speed of 12 m/s. A hub height of 50 m was assumed. The results in Fig. 9 show that the results are all under-estimated, due to the under-estimations of wind speeds in the most frequent sectors. The under-estimation is quite consistent for all models (between 10% and 15%) except E-Wind, which under-estimates the AEP by 24%.

Details of the variations of the AEP for each wind direction sector can be found in Barber et al. (2001). It was found that the AEP is significantly under-predicted in the most frequent sector (240°), leading to an overall under-prediction of AEP. There is no particular pattern in the variation of AEP between each workflow. The very small effect of flow turning on the WF-4 and WF-5a (Fluent) results can be seen for some sectors.

4.4 Site 4

For this site, the AEP has been calculated at the validation location using the power curve of the Enercon E-82 wind turbine. This wind turbine has a rated power of 2 MW and a rated wind speed of 12.5 m/s. The hub height is 78 m. The results in Fig. 10 show that, as opposed to the Site 3, the results for Site 4 are all over-estimated, due to the over-estimations of wind speeds in the most frequent sectors. The over-estimation is largest for WF-4 (Fluent RANS), and the SBES simulation in WF-5a reduce this slightly. The effect of flow turning is minimal. The over-estimation is small for WF-1 (WindPro) and WF-2 (WindSim).

Details of the variations of the AEP for each wind direction sector can be found in Barber et al. (2001). It was found that the large over-prediction in AEP by the WF-3 and WF-4 workflows mainly occurs because of the over-prediction in the 240° sector, because this is the most frequently occurring sector. Additionally, it was found that an under-prediction of WF-1 (WindPro) and WF-2 (WindSim) in the 210° sector is probably compensated for by the over-prediction in 240°, because both of these sectors occur for a similar proportion of time.

4.5 Site 5

For this site, the AEP has been calculated at the validation location using the power curve of the planned wind turbine type. The results shown in Fig. 11 match very well for WF-4T (Fluent RANS) and WF-5aT (Fluent SBES), with deviations less than 6%. The WF-1 (WindPro) and WF-2 (WindSIM) results are significantly lower, with deviations of 30% and 26%, respectively. These deviations may initially be surprising, considering that the wind profile RMSE values between simulations and measurements for the four workflows are similar. However, this has occurred because both under-predictions and over-predictions of the wind speed lead to a positive RMSE, whereas a combination of over-predicted and under-predicted wind speeds cancel each other out for the AEP calculation.

Details of the variations of the AEP for each wind direction sector can be found in Barber et al. (2001). It was found that shows that the AEP is particularly under-predicted in the 210° sector for all workflows, and in the 240° sector for WF-1 and WF-2, but not for WF-4T and WF-5aT. Thus, the large difference in workflow results is attributed to the strongly under-

https://doi.org/10.5194/wes-2021-158
Preprint. Discussion started: 19 January 2022

predicted wind speed in the 240° sector of WindPro and WindSim. This has such a large influence on the AEP because of the very high average wind speeds in this sector combined with the high frequency of occurrence. It reveals an important point about this work – that the average absolute difference in wind speed over all sectors cannot be used as a reliable metric for the expected difference in AEP, even when it is weighted for the frequency of occurrence.

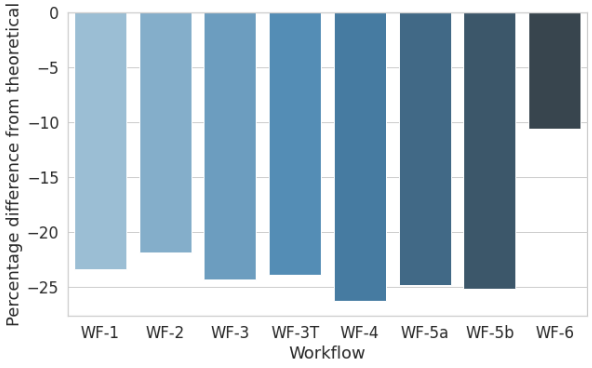

Figure 7. Site 1 - Percentage difference in gross AEP from the 'theoretical' value for each workflow applied

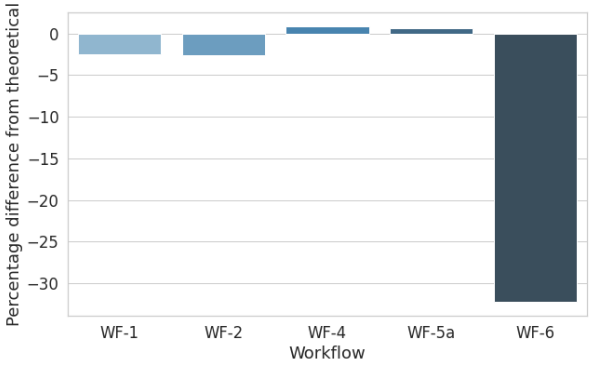

Figure 8. Site 2 - Percentage difference in gross AEP from the 'theoretical' value for each workflow applied

https://doi.org/10.5194/wes-2021-158
Preprint. Discussion started: 19 January 2022

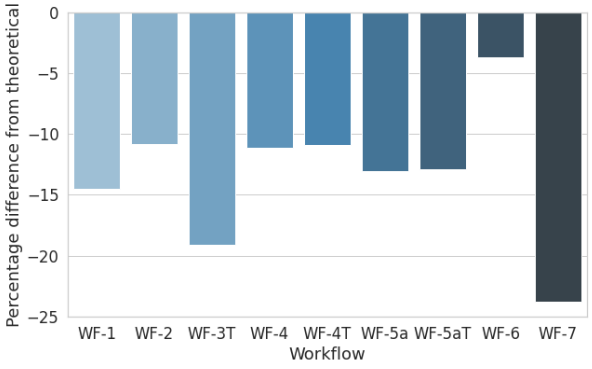

Figure 9. Site 3 - Percentage difference in gross AEP from the 'theoretical' value for each workflow applied

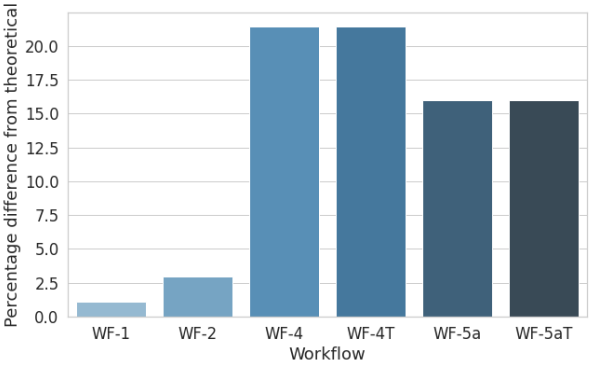

Figure 10. Site 4 - Percentage difference in gross AEP from the 'theoretical' value for each workflow applied

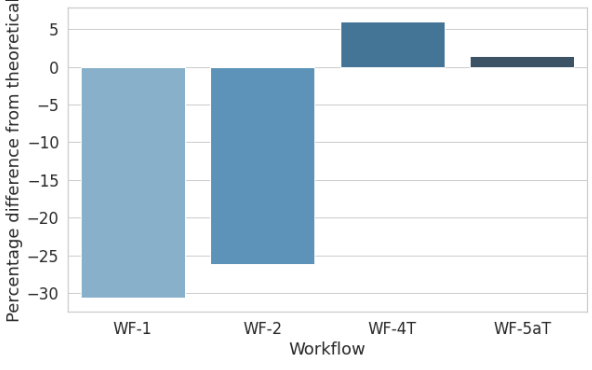

Figure 11. Site 5 - Percentage difference in gross AEP from the 'theoretical' value for each workflow applied

https://doi.org/10.5194/wes-2021-158
Preprint. Discussion started: 19 January 2022

eawe european academy of wind energy
Open Access WIND ENERGY SCIENCE DISCUSSIONS

4.6 Comparison of wind speed and AEP results

In this section, the results of the simulated wind speeds and AEP calculations are compared by plotting the error in simulated wind speeds against the error in expected AEP at the validation location for each site (Fig. 12). Each row corresponds to one site (from Site 1 to Site 5). The left-hand plots show the average error of all 12 wind speed direction sectors using a simple average, whereas the right-hand plots show the average error of all 12 wind speed direction sectors using an average weighted with wind speed frequency.

Generally, the correlation between wind speed error and AEP error is fairly low quality, and R^2 ranging from 0.0123 to 0.559 for Sites 1, 2, 3 and 5. The exception is Site 4, which has R^2 = 0.94 for simple averaging and 0.95 for weighted averaging. The authors could find no particular reason why Site 4 should result in this significantly better correlation, except for the seemingly coincidental combination of a wide range of different effects that have come together to produce this result.

The weighting does not have a large effect on the correlation coefficients, and in some cases actually reduces the values. This indicates that the absolute value of the wind speed has a larger effect on the AEP accuracy than the actual accuracy in each sector, and can be explained by the cubic relationship between wind speed and power.

For four out of five sites, there is no clear relationship between wind speed error and overall AEP error. Wind profile prediction accuracy does not translate directly or linearly to AEP accuracy. This is firstly because there is a surprisingly large variation in energy production calculations between tools, and secondly because the AEP depends strongly upon the relative strength and occurrence of the wind speed in the most commonly-occurring wind direction sectors. This means that the wind model that produces the most accurate wind predictions for a certain wind direction over a certain time period does not always result in the most suitable model for the AEP estimation of a given complex terrain site. In fact, the large number of steps within the WRA process often lead to the choice of wind model being less important for the overall WRA accuracy than would suggest by only looking at wind speeds. Not only this, but additionally it is not immediately obvious which sites have a high correlation and which ones do not.

It is therefore concluded that it is vitally important for researchers to consider overall AEP - and all the steps towards calculating it - when evaluating simulations of flow over complex terrain. This agrees with similar recent qualitative findings from the CREYAP2021 study[7].

[7]https://windeurope.org/tech2021/creyap-2021/

https://doi.org/10.5194/wes-2021-158
Preprint. Discussion started: 19 January 2022

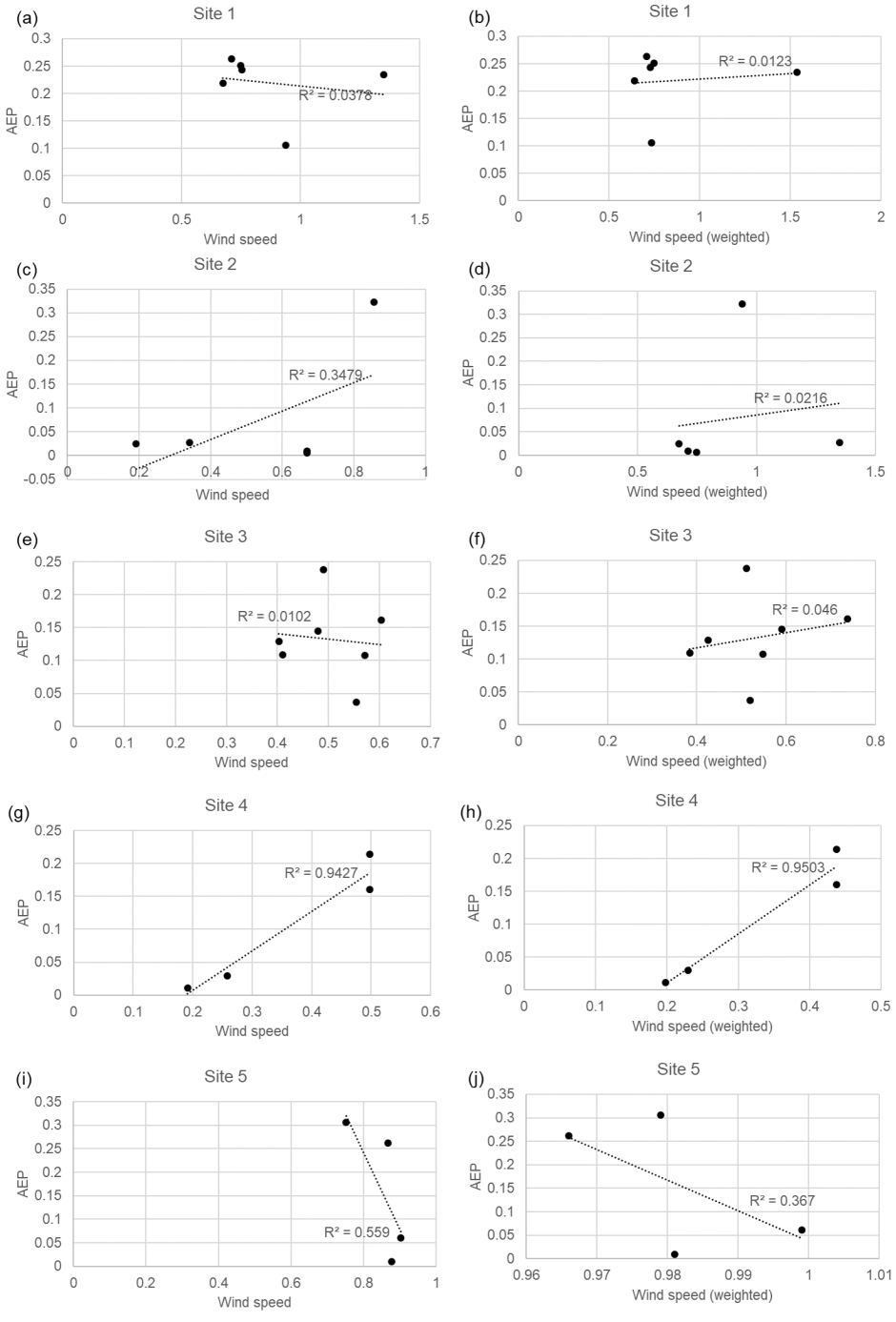

Figure 12. Comparison of AEP errors to wind speed errors for all workflows and all sites (left: AEP compared to simple average wind speed; right: AEP compared to wind speed weighted for wind speed frequency

https://doi.org/10.5194/wes-2021-158
Preprint. Discussion started: 19 January 2022

5 Conclusions

A range of simulations have been carried out with seven different wind modelling tools at five different complex terrain sites and the results compared to wind speed measurements at validation locations. This was then extended to AEP estimations (without wake effects), and it was found that wind profile prediction accuracy does not translate directly or linearly to AEP accuracy. This is firstly because there is a surprisingly large variation in energy production calculations between tools, and secondly because the AEP depends strongly upon the relative strength and occurrence of the wind speed in the most commonly-occurring wind direction sectors. This means that the wind model that produces the most accurate wind predictions for a certain wind direction over a certain time period does not always result in the most suitable model for the AEP estimation of a given complex terrain site. In fact, the large number of steps within the WRA process often lead to the choice of wind model being less important for the overall WRA accuracy than would suggest by only looking at wind speeds. It is therefore vitally important for researchers to consider overall AEP - and all the steps towards calculating it - when evaluating simulations of flow over complex terrain.

https://doi.org/10.5194/wes-2021-158
Preprint. Discussion started: 19 January 2022

Author contributions. Sarah Barber managed and coordinated the project and was responsible for writing the paper. Alain Schubiger carried out the Fluent simulations and developed the script for the AEP calculation process. Sara Koller and Dominik Eggli carried out the WindPro, WindSim and PALM simulations. Alexander Radi carried out the E-Wind simulations. Andreas Rumpf carried out the CFX simulations and developed the script for the AEP calculation process. Hermann Knaus supervised the work of Andreas Rumpf and provided valuable inputs for the paper.

Competing interests. There are no competing interests

Acknowledgements. This work was carried out as part of the projects "A new process for the pragmatic choice of wind models in complex terrain" funded by the Swiss Federal Office of Energy (SI/501807-01) and the German Federal Environmental Foundation (34933/01). Thanks also to the partner companies of this project for providing data and inputs about the simulated sites, including ewz, ADEV, Enercon as well as the Institut für Flugzeugbau at the Universität Stuttgart for providing us with the lidar data from the "Lidar complex" project.

https://doi.org/10.5194/wes-2021-158
Preprint. Discussion started: 19 January 2022

eawe european academy of wind energy
Open Access WIND ENERGY SCIENCE DISCUSSIONS

References

Alletto, M., Radi, A., Adib, J., Langner, J., Peralta, C., Altmikus, A., and Letzel, M.: E-Wind: Steady state CFD approach for stratified flows used for site assessment at Enercon, Journal of Physics: Conference Series, 1037, 072 020, https://doi.org/10.1088/1742-6596/1037/7/072020, 2018.

Bao, J., Chow, F. K., and Lundquist, K. A.: Large-Eddy Simulation over Complex Terrain Using an Improved Immersed Boundary Method in the Weather Research and Forecasting Model, Monthly Weather Review, 146, 2781 – 2797, https://doi.org/10.1175/MWR-D-18-0067.1, 2018.

Barber, S., Schubiger, A., Koller, S., Eggli, D., Rumpf, A., and Knaus, H.: A new process for the pragmatic choice of wind models in complex terrain, final report, Eastern Switzerland University of Applied Sciences, https://drive.switch.ch/index.php/s/DGxWeKQ35nnbPMW, 2001.

Barber, S., Buehler, M., and Nordborg, H.: IEA Wind Task 31: Design of a new comparison metrics simulation challenge for wind resource assessment in complex terrain Stage 1, Journal of Physics: Conference Series, 1618, 062 013, https://doi.org/10.1088/1742-6596/1618/6/062013, 2020a.

Barber, S., Schubiger, A., Koller, S., Rumpf, A., Knaus, H., and Nordborg, H.: Actual Total Cost reduction of commercial CFD modelling tools for Wind Resource Assessment in complex terrain, Journal of Physics: Conference Series, 1618, 062 012, https://doi.org/10.1088/1742-6596/1618/6/062012, 2020b.

Bechmann, A., Sørensen, N. N., Berg, J., Mann, J., and Réthoré, P.-E.: The Bolund Experiment, Part II: Blind Comparison of Microscale Flow Models, Boundary-Layer Meteorology, 141, 245–271, https://doi.org/10.1007/s10546-011-9637-x, 2011.

Berg, J., Mann, J., Bechmann, A., Courtney, M. S., and Jørgensen, H. E.: The Bolund Experiment, Part I: Flow Over a Steep, Three-Dimensional Hill, Boundary-Layer Meteorology, 141, 219–243, https://doi.org/10.1007/s10546-011-9636-y, 2011.

Bowen, A. J. and Mortensen, N. G.: Exploring the limits of WAsP the wind atlas analysis and application program, in: European Union wind energy conference, edited by Zervos, A., Ehmann, H., Helm, P., and Stephens, H. S., Bedford: H.S. Stephens & Associates, 1996.

Knaus, H., Rautenberg, A., and Bange, J.: Model comparison of two different non-hydrostatic formulations for the Navier-Stokes equations simulating wind flow in complex terrain, Journal of Wind Engineering and Industrial Aerodynamics, 169, 290–307, https://doi.org/https://doi.org/10.1016/j.jweia.2017.07.017, 2017.

Lee, J. C. Y. and Fields, M. J.: An overview of wind-energy-production prediction bias, losses, and uncertainties, Wind Energy Science, 6, 311–365, https://doi.org/10.5194/wes-6-311-2021, 2021.

Liu, J., Chen, J. M., Black, T. A., and Novak, M. D.: E-ϵ modelling of turbulent air flow downwind of a model forest edge, Boundary-Layer Meteorology, 77, 21–44, 1996.

Menke, R., Vasiljević, N., Mann, J., and Lundquist, J. K.: Characterization of flow recirculation zones at the Perdigão site using multi-lidar measurements, Atmospheric Chemistry and Physics, 19, 2713–2723, https://doi.org/10.5194/acp-19-2713-2019, 2019.

Menter, F.: Zonal Two Equation k-w Turbulence Models For Aerodynamic Flows, 2012.

Montavon, C.: Validation of a non-hydrostatic numerical model to simulate stratified wind fields over complex topography, Journal of Wind Engineering and Industrial Aerodynamics, 74-76, 273–282, https://doi.org/https://doi.org/10.1016/S0167-6105(98)00024-5, 1998.

Mortensen, N., Nielsen, M., and Ejsing Jørgensen, H.: Comparison of Resource and Energy Yield Assessment Procedures 2011-2015: What have we learned and what needs to be done?, in: Proceedings of the EWEA Annual Event and Exhibition 2015, European Wind Energy

https://doi.org/10.5194/wes-2021-158
Preprint. Discussion started: 19 January 2022

Association (EWEA), paper for poster presentation; EWEA Annual Conference and Exhibition 2015 ; Conference date: 17-11-2015 Through 20-11-2015, 2015.

Pozo, J. M., Geers, A. J., Villa-Uriol, M.-C., and Frangi, A. F.: Flow complexity in open systems: interlacing complexity index based on mutual information, Journal of Fluid Mechanics, 825, 704–742, https://doi.org/10.1017/jfm.2017.392, 2017.

Richards, P. and Hoxey, R.: Appropriate boundary conditions for computational wind engineering models using the k- turbulence model, Journal of Wind Engineering and Industrial Aerodynamics, 46-47, 145–153, https://doi.org/https://doi.org/10.1016/0167-6105(93)90124-7, proceedings of the 1st International on Computational Wind Engineering, 1993.

Rodi, W. and Spalding, D.: PAPER 2 - A Two-Parameter Model of Turbulence, and its Application to Free Jets, in: Numerical Prediction of Flow, Heat Transfer, Turbulence and Combustion, edited by Patankar, S. V., Pollard, A., Singhal, A. K., and Vanka, S. P., pp. 22–32, Pergamon, https://doi.org/https://doi.org/10.1016/B978-0-08-030937-8.50010-6, 1983.

Sayre, R., Frye, C., Karagulle, D., Krauer, J., Breyer, S., Aniello, P., Wright, D. J., Payne, D., Adler, C., Warner, H., VanSistine, D. P., and Cress, J.: A New High-Resolution Map of World Mountains and an Online Tool for Visualizing and Comparing Characterizations of Global Mountain Distributions, Mountain Research and Development, 38, 240 – 249, https://doi.org/10.1659/MRD-JOURNAL-D-17-00107.1, 2018.

Schulz, C., Klein, L., Weihing, P., Lutz, T., and Krämer, E.: CFD Studies on Wind Turbines in Complex Terrain under Atmospheric Inflow Conditions, Journal of Physics: Conference Series, 524, 012 134, https://doi.org/10.1088/1742-6596/524/1/012134, 2014.

Wiernga, J.: Representative roughness parameters for homogeneous terrain, Boundary-Layer Meteorology, 63, 323–363, 1993.

Wood, N.: The onset of separation in neutral, turbulent flow over hills., Boundary-Layer Meteorology, 76, 137–164, 1995.